

Multidither adaptive optical systems based on wave-front sensor with spatially separated control channels

A.N. Alikhanov, E.A. Berchenko, V.Yu. Kiselev, V.N. Kuleshov, S.N. Larin, E.A. Narusbek, B.V. Prilepskii, V.G. Son, and A.S. Filatov

*SOLTO Special Design Bureau,
State Unitary Branch Enterprise of Astrofizika Scientific and Production Association, Moscow*

Received August 26, 2004

This paper presents the results of theoretical and experimental investigation into adaptive optical systems (AOSs) based on a wave-front sensor with spatially separated control channels. The main feature of such systems consists in the fact that signals received by each photodetector can be directly used for control of deformable mirror (DM) actuators. For this purpose, light wave phase modulation at the same frequency for the entire wave front (WF) is used. A multi-element photodetector is placed in the plane, optically conjugate with a phase corrector of the optical system. That is why such systems seem analogous, to some extent, to aperture sounding (multidither) systems. Theoretical analysis has shown that two variants of the adaptive optical systems based on wave-front sensor (WFS) with spatially separated control channels are possible. The first one involves phase modulation directly in the corrector plane. The second one involves phase modulation in the focal plane of the WFS objective. In both of these cases, the signal from a photodetector is equal to zero, if the WF local curvature in the corresponding region is also zero. Such WFS are often referred to as curvature sensors. It is shown that stability of adaptive optical systems based on wave-front sensor with spatially separated control channels and phase modulation in the corrector plane strongly depends on the WF tilts. But their sensitivity (for equal focal lengths) is much higher than that of the AOSs with phase modulation in the focal plane of the WFS objective. The laboratory setup used for experimental study of the adaptive optical systems based on wave-front sensor with spatially separated control channels is described. In this setup, we used deformable mirrors with correspondingly 7 and 37 PZT actuators of special type. One of the features of these actuators was the existence of two sections: the control section and the modulation one. To study the operation of AOS with phase modulation in the focal plane of the WFS objective, we used special design of phase modulators.

Introduction

An adaptive optical system, employing a wave-front sensor referred to as an optical processor, was described in Ref. 1. A key element of this wave-front sensor is a deformable mirror with a variable curvature, whose vertex is located in the focal plane of the sensor objective. The mirror curvature varies in time, for example, by the harmonic law. The signal from a multi-element light detector, after the synchronous detection and amplification, is directly used to control the corrector of the adaptive optical system. The corrector and detector are located in the optically conjugate planes, and the arrangement of the photosensitive areas of the detector elements copies (with the appropriate magnification) the arrangement of the actuators on the corrector surface. An adaptive optical system operated following analogous principles was described in Ref. 2.

The analysis performed in Ref. 3 showed that the method of measurement of wave front distortions in the sensors of the adaptive optical systems described in Refs. 1 and 2 can be considered as a version of the multidither (aperture sounding) method, which was used by O'Meara in the 1970s to correct atmospheric distortions in multichannel coherent transmitting optical systems.⁴

The main distinction of the systems described in Refs. 1 and 2 from the early multidither systems is that the latter ones used multifrequency phase modulation of the light wave in the entrance pupil. The signal was measured with a single-element detector, having a photosensitive area with the size nearly equal to diffraction-limited pixel size, located at the focus of the receiving objective, and the control signal was separated by means of radio methods in the corresponding channels.

In Ref. 3 it was noted that there are two versions of construction of multidither systems with the spatially separated control channels. In the first version, the phase modulation of the light wave (at a single frequency) at every wave front point is created, as in the early multidither systems, directly on the corrector (in the entrance pupil of the sensor). In the second version, the phase modulation of the light wave is being done in the exit pupil of the sensor (in the detector plane) by changing the parameters of a phase modulator, set in the focal plane of the sensor objective (a mirror with variable curvature in Refs. 1 and 2).

In this paper, we present the main theses of Ref. 3, which suggest the similarity of the early multidither systems and the systems described in Refs. 1 and 2.

Wave-front sensors for multidither systems with modulation on the corrector will be referred to as

type I sensors, while those with phase modulation in the plane, where the detector photosensitive areas are set, will be referred to as type II sensors.

1. Wave-front sensors for multidither adaptive optical systems with spatially separated channels

Figure 1 depicts the general optical arrangement of a wave-front sensor for multidither adaptive optical systems with spatially separated channels. The wave front corrector is assumed to be located at the entrance pupil of the sensor optical system. The point $\rho \{ \xi, \eta \}$ of the entrance pupil corresponds to the point $\rho' \{ \xi', \eta' \}$ in the exit pupil, where a multi-element detector is set. Introduce the coordinate system $r(x, y)$ in the focal plane. Assume that an amplitude–phase filter with the transmission function $T(r)$ is set in the focal plane of the optical system.

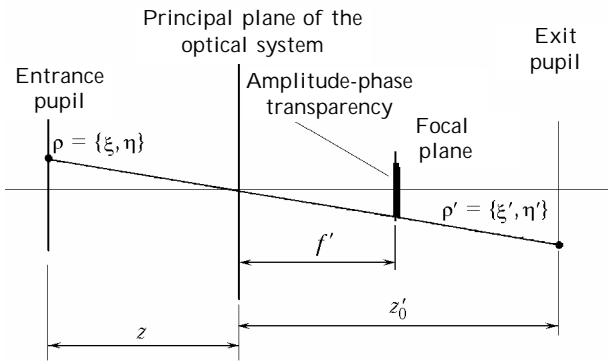


Fig. 1.

Accurate to insignificant phase factors, the distribution of the light wave field in the exit pupil for an infinitely remote point source can be calculated as

$$E_{out}(\rho') = \frac{\beta}{\lambda^2 f'^2} \int_{\rho} E_{in}(\rho) H(\rho + \beta\rho') d^2\rho,$$

where λ is the radiation wavelength; f' is the equivalent focal length of the optical system of the objective of the wave-front sensor; $1/\beta$ is the magnification of the optical system of the wave-front sensor in the pupils; $H(\rho + \beta\rho')$ is the transfer function of the wave-front sensor

$$H(\rho + \beta\rho') = \int_r T(r) \exp\left[-\frac{ik}{f'} r(\rho + \beta\rho')\right] d^2r,$$

$k = 2\pi/\lambda$ is the wave number.

The features of signals at the modulation frequency in type I and type II wave-front sensors with the spatially separated channels have been analyzed in Ref. 5 with the allowance for the alignment imperfections in optical elements of these sensors. The analysis was carried out for the case that the light wave field in the entrance pupil is specified in the form

$$E_{in}(\rho) = \exp[ik\Delta(\rho)];$$

$$\Delta(\rho) = \begin{cases} -\alpha_x(\xi - \xi_0) - \alpha_y(\eta - \eta_0) + \\ + \Delta \left(1 - \frac{(\xi - \xi_0)^2 + (\eta - \eta_0)^2}{\rho_0^2} \right) & \text{at } \rho \leq \rho_0, \\ 0 & \text{at } \rho > \rho_0, \end{cases}$$

where $\alpha = \{ \alpha_x, \alpha_y \}$ are wave front tilts; ρ_0 is the spatial scale of wave front distortions; Δ is the maximum wave front deformation at the point with coordinates $\rho_0 = \{ \xi_0, \eta_0 \}$. The wave front curvature q is related to the maximum deformation Δ and the spatial scale ρ_0 as $q = 2\Delta/(\rho_0^2)$. It was assumed that the photosensitive areas of light detectors of the adaptive system are far from the boundary of the exit pupil.

For type I sensors, the transparency of the phase modulator was determined as

$$T(r) = \exp[-r^2/(2r_0^2)],$$

and $q \rightarrow q(\Delta) + qm \sin(\omega t)$. For type II sensors, the transparency of the phase modulators was specified in the form

$$T(r, t) = \exp(ikqm(t)r^2/2),$$

where $qm(t) = qm \sin(\omega t)$.

The features of the signals, carrying the information about wavefront distortions, will be studied by investigating the behavior of the function

$$S(q) = \frac{I_1(q)}{I(0,0)} \cdot 100\%,$$

where $I(q, t)$ is the radiation intensity at the photosensitive area of photodetectors as a function of the wave front curvature q ; $I_1(q)$ is the amplitude of the first harmonic in the spectrum of the function $I(q, t)$.

In Ref. 5, it was shown that the signals at the modulation frequency from the output of the type I sensors have the following features.

1. If the center of a photodetector sensitive area coincides with the image of a point ρ_0 , then at $q(\Delta) = 0$ the signal is zero irrespective of the wave front tilt.

2. If the center of a photodetector sensitive area does not coincide with the image of a point ρ_0 , then the signal is nonzero in the presence of a wave front tilt and at $q(\Delta) = 0$. The signal value depends on the errors in alignment of the detectors and actuators of the deformable mirror, on the wave front tilt, and on the modulation amplitude q . The signal is zero, if wave front tilts are zero.

3. If the center of a photodetector sensitive area coincides with the image of a point ρ_0 , then the steepness S of the dependence of the signal at the

modulation frequency on the local wave front curvature $q(\Delta)$ depends on the wave front tilt. In this case, the change of the tilt may lead to the alternation of the sign of the steepness S .

In the general case, the sign of the steepness S is determined by the shift αs , which, in its turn, is determined as

$$\alpha s = \sqrt{(\delta r q)^2 + 2\delta r q \alpha \cos \Psi + \alpha^2},$$

where δr is the shift of the photodetector center from the point with the coordinates $\{\xi_0, \eta_0\}$; Ψ is the angle between the vectors

$$\{\delta \xi, \delta \eta\} = \{\xi + \beta \xi', \eta + \beta \eta'\}$$

and α . The alternation of the steepness sign leads to the structure instability in the closed loop of the adaptive system. For the system to be stable, the following condition should be satisfied

$$\alpha s < \frac{r_0}{f'} \sqrt{1 + \left(\frac{f' q(\Delta)}{k r_0^2} \right)^2} \approx \frac{r_0}{f'}$$

For the adaptive systems with type II sensors, the signal from the detector output for the internal points of the exit pupil is independent of wave front tilts being only determined by the local curvature. However, for detection of signals at the modulation frequency, comparable with the signals detected from the output of the type I sensors (at equal objective focal lengths), much higher (~100 times) modulation amplitudes $qm(t)$ are needed.

2. Newtonian phase modulator

The design of a wave-front sensor with a Newtonian phase modulator is shown in Fig. 2. A plane-convex lens 2 with a parallel-sided plate 3, pressed to its top, is set in the focal plane of the sensor objective 1. A piezoceramic (unimorph) plate 4 with an aperture at the center is glued to another side of the parallel-sided plate. The aperture size is much larger than the diffraction-limited pixel size and equal to several millimeters. The modulating voltage is applied to the piezoceramic plate. The parameters of the lens 2 are such that it constructs the image of the exit pupil (deformable mirror of the adaptive system) in the plane 5, in which the sensitive areas of the sensor photodetector are located.

The working surface area of the Newtonian phase modulator is a small contact zone between the plate and the lens, having the size about 100–200 μm at the optical parameters of the wave-front sensor, given in the next Section. We have no exact quantitative description of variations in the optical signal propagated through this area. However, for multidither systems, in which the signals at the modulation frequency are nulled upon the compensation for wave front distortions and are not used for reconstruction of the wave front, there is no need in such a description.

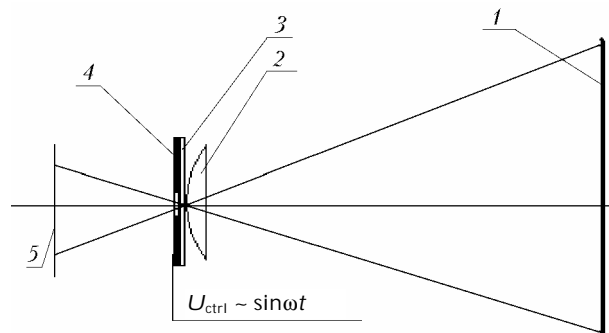


Fig. 2. Newtonian phase modulator.

We performed the qualitative analysis of the operation of this modulator, assuming that, in the working area of the Newtonian phase modulator, the focal power of the "lens–parallel-sided plate" sandwich varies by the law

$$q(r) = q_c + (q_0 - q_c) \left[1 - r^{2p} \exp\left(-\frac{r^2}{2r_0^2}\right) \right],$$

where r is the distance from the lens top to the considered point in the objective focal plane; r_0 is the parameter, characterizing the size of the contact zone between the lens and the parallel-sided plate; q_c is the focal power of the phase modulator at the center of the contact zone; p is the parameter, determining the properties of the model of the Newtonian phase modulator; q_0 is the focal power of the lens. Since the lens with the focal power q_0 together with the sensor objective transfers, with the given magnification, the surface of the plane of the corrector deformable mirror onto the plane, in which the photodetector sensitive areas are located, it can be believed that the transparency of the Newtonian phase modulator for the chosen model is described by the equation

$$T(r) = \exp\left[-i \frac{k \delta q r^{2(p+1)}}{2} \exp\left(-\frac{r^2}{2r_0^2}\right)\right],$$

where $\delta q = q_0 - q_c$. As the modulating voltage is applied to the unimorph of the Newtonian phase modulator, both of the modulator parameters (r_0 and δq) can vary in the general case, and the curves obtained for the characteristic $S(q)$ are quite variable.

The observed experimental behavior of the adaptive system with such a wave-front sensor can be explained qualitatively, if the characteristic $S(q)$ has the form shown in Fig. 3. The curve on the right in this figure shows in more detail the behavior of the function $S(q)$ in the region of zero values of the local wave front curvature near an individual detector, while the curve on the left shows this function in a wider region of variation of the local curvature. It can be seen that, in the region of zero values of the local curvature, the signals at the modulation frequency are zero, and at $q = 0$ we have a point of inflection of the curve. To the right and to the left from the zero local curvature, there are two points, for which $S(q) = 0$. At high distortions of the wave front $S(q) \rightarrow 0$.

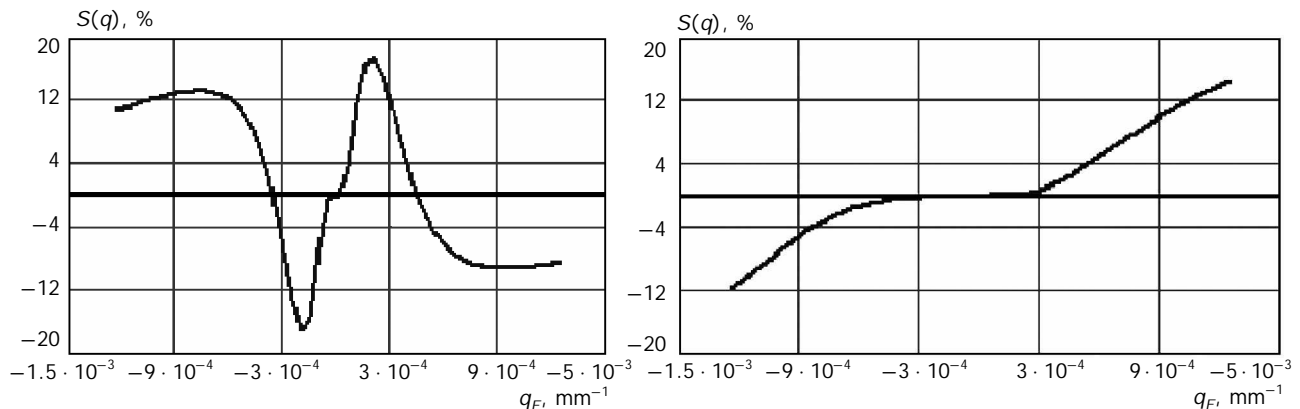


Fig. 3. Typical model modulation characteristics of the Newtonian phase modulator.

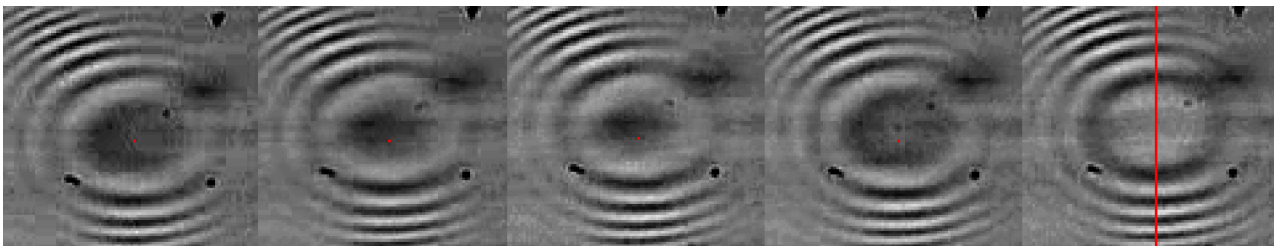


Fig. 4.

In the photos of the Newtonian phase modulator (Fig. 4), obtained with its illumination by diffuse light, we can see a characteristic system of fringes of the interference pattern. Different photos correspond to different voltages applied to the phase modulator.

It can be seen that the view of the central area changes upon the voltage variation.

Figure 5 shows the image of the Newtonian phase modulator, illuminated by two light sources. One of these sources is a diffuse beam, giving the system of Newtonian interference fringes, while another corresponds to the radiation of a gas laser, focused onto the contact zone between the lens and the parallel-sided plate.

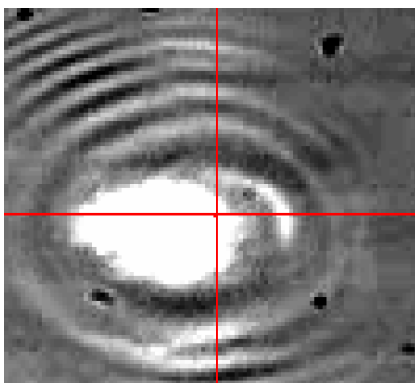


Fig. 5.

The illumination of the phase modulator by a focused laser radiation does not create a system of interference fringes, characteristic of the illumination with diffuse light.

3. Laboratory setup for investigation of multidither adaptive optical systems with spatially separated channels

Figure 6 shows optical arrangement of the laboratory setup for investigation of the multidither adaptive optical systems based on wave-front sensors with spatially separated channels. Figure 7 shows the general view of the setup.

A standard Mark IV interferometer served a source of the collimated light beam. A bimorph deformable mirror directed the light beam 80 mm in diameter to the wave-front sensor.

The bimorph deformable mirror (Fig. 8), having 32 active zones at the clear aperture of 180 mm, was used in the laboratory setup as an imitator of atmospheric distortions of the radiation wave front. The membrane of this mirror has a thickness of 2.5 mm and is made of silicon. This mirror was capable of creating both static and dynamic distortions, which were then compensated for by the adaptive system.

The reflecting surface of the deformable mirror–corrector (Fig. 9) is located in the entrance pupil of the sensor optics behind the imitator of distortions. The normal to the mirror makes the angle of 10° with the optical axis of the sensor.

The mirror–corrector is a 2-mm thick silicon membrane, which is deformed by 37 separate column piezoactuators (Fig. 10).

To carry out experiments with type I multidither adaptive optical systems, every actuator was made in the form of two sections (large and small), which were controlled separately.

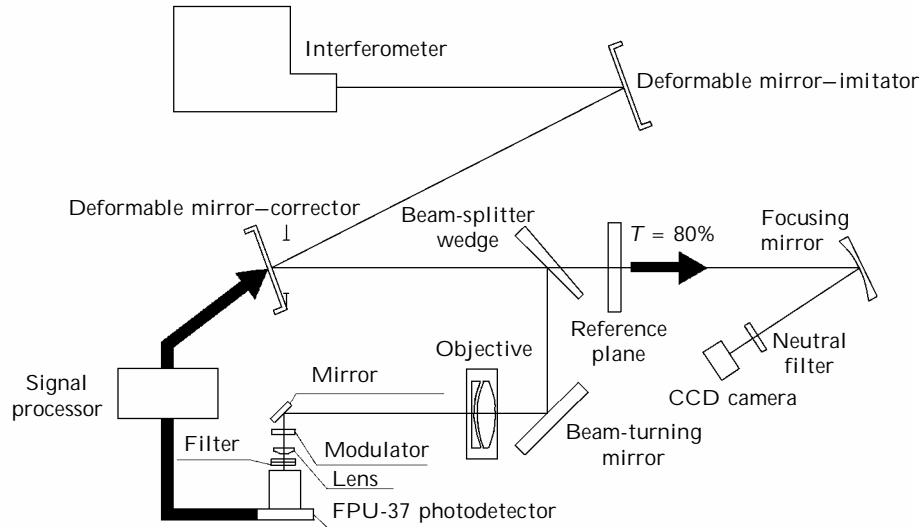


Fig. 6. Optical arrangement of the laboratory setup for investigation of multidither adaptive optical systems with spatially separated channels.

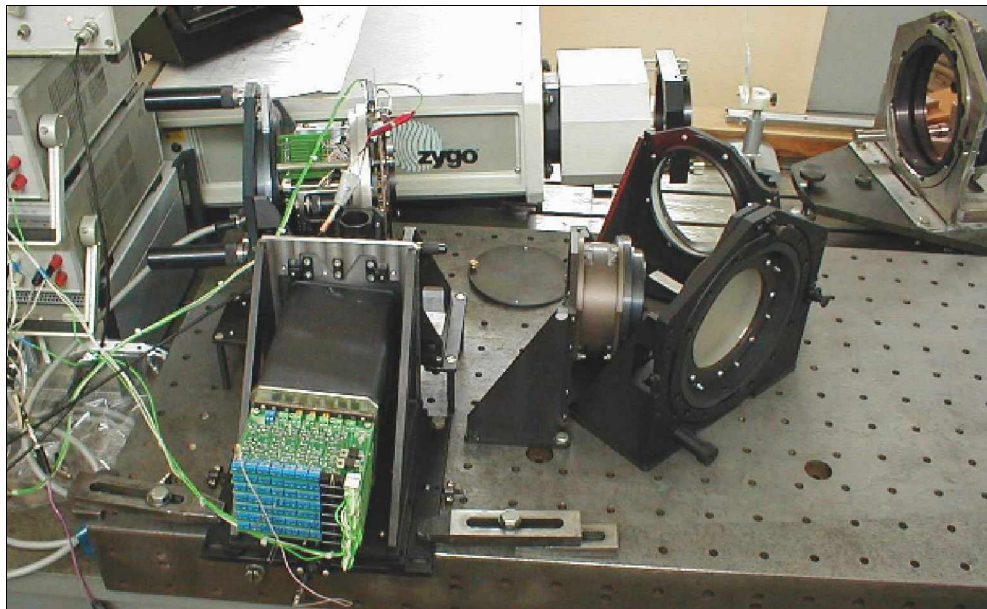


Fig. 7. General view of the laboratory setup.



Fig. 8. Bimorph mirror for imitation of wave front distortions.



Fig. 9. Deformable mirror-corrector.

The longer section is used for the correction of wave front distortions, while the shorter section of the piezoactuator is used for phase modulation of the wave front. The arrangement of the actuators on the mirror surface is shown in Fig. 11.

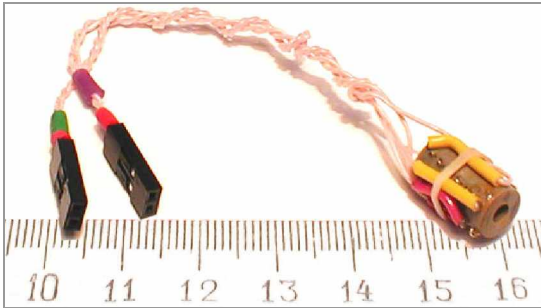


Fig. 10. Column piezoactuator of the deformable mirror-corrector.

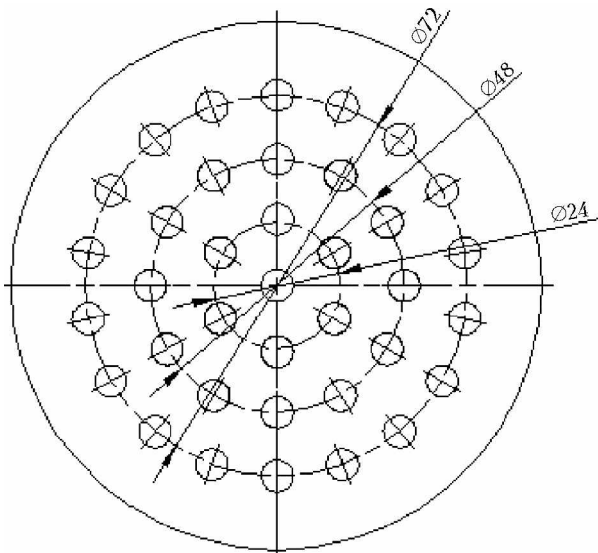


Fig. 11. Arrangement of the actuators on the surface of the deformable mirror-corrector.

The parameters of the deformable mirrors for correction and imitation of wave front distortions are tabulated below.

Parameter	For correction	For imitation
Free aperture, mm	Ø 80	Ø 180
Membrane material	Single-crystalline silicon	Single-crystalline silicon
Membrane thickness, mm	2	2.5
Geometry of actuator arrangement	3 rings at Ø 72 mm	3 rings at Ø 160 mm
Actuator type	PZT	PZT
Maximum local deformation at the longer section ($U_{ctrl} = \pm 200$ V), μm	± 2	—
Maximum local deformation at the shorter section ($U_{ctrl} = \pm 20$ V), μm	± 0.05	—
Maximum local deformation of bimorph ($U_{ctrl} = \pm 200$ V), μm	—	2.5
Frequency of first resonance, kHz	~1	—
Maximum operating frequency, Hz	80	30

The light reflected by the corrector is incident onto the beam-splitter wedge, which transmits 80% of the light to the long-focus mirror, forming the light distribution for control of the quality of adaptive system operation, and reflects 20% of the light to the beam-turning mirror of the wave-front sensor (see Fig. 6).

The beam-turning mirror is followed by the objective, in front of whose focal plane a plane mirror is installed, which directs the light to the phase modulator of the wave-front sensor. The lens located behind the phase modulator constructs the image of the entrance (exit) pupil plane with the given magnification. The input ends of optical fibers of the unit, being a part of the FPU-37 photodetector, are located in the plane of the exit pupil. Every monofiber is coupled with a detector of the photodetector array.

To decrease the light losses because of the loose filling of the exit pupil by the fibers, the fiber core 600 μm in diameter was made of the glass with the high refractive index, and the glass cladding of the fiber has the thickness of about 10 μm . Figure 12 shows the general view of the fiber unit design and the view of the fiber unit during the propagation of the laser radiation through it.

The signals from the detector outputs pass through narrow-band filters, tuned at the modulation frequency $f = 2$ kHz. The signals, carrying the information about distortions of the wave front phase in each of 37 control zones, are separated from the filtered signals by the method of synchronous detection. After integration, these signals are amplified by high-voltage amplifiers and applied to the appropriate corrector actuators so that the negative feedback exists in the closed loop. The joint action of the corrector and the control system results in the correction of the wave front of the working radiation.

The light beam quality in the experiments was controlled by two methods. First, a CCD camera recorded the light distribution in the focal plane of the long-focus ($F = 6.25$ m) mirror. Second, the interference pattern of the light beam was recorded returned into the interferometer by the reference plane set at the exit of the adaptive system.

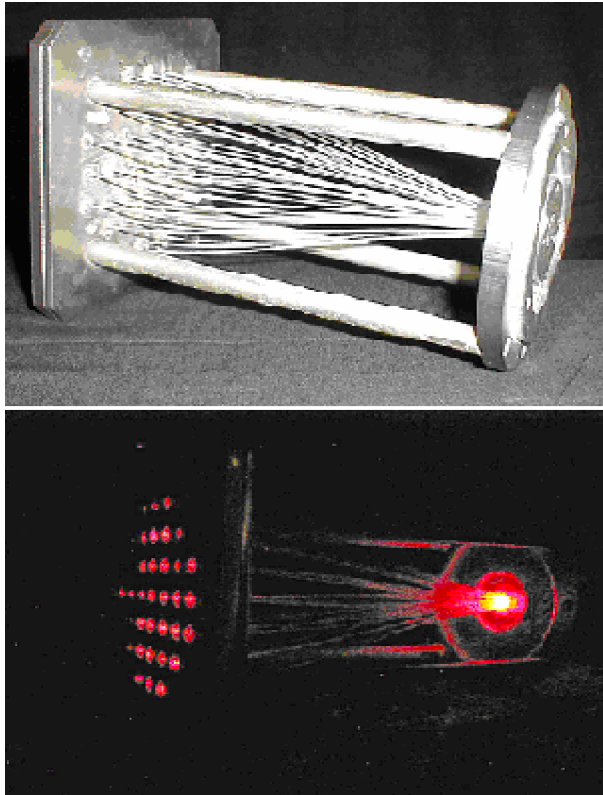


Fig. 12. Optical fiber unit of the wave-front sensor.

The parameters of the optical system of the wave-front sensor used in the laboratory mockup are presented below.

Entrance pupil diameter, mm.....	80
Separation of the entrance pupil from the first surface of the objective, mm.....	325
Objective focal length, mm.....	300
Magnification in pupils.....	1/12
Diameter of the spot, containing 84%, of radiation energy, in the focal plane, μm	10
Working radiation wavelength, μm	0.63

4. Results

4.1. Type I multidither system

In studying type I multidither adaptive optical systems, 50 and 100 μm point diaphragms were used as amplitude modulators (SLM).

For the effective modulation of the surface of the deformable mirror–corrector, neighboring actuators should move in anti-phase. However, the used arrangement of actuators on the mirror surface does not allow realization of this. Therefore, the sign of the shift amplitude during the modulation alternated from one ring to another. The mirror shape during the modulation had the form shown in Fig. 13.

The experiments have demonstrated that the modulation characteristic of the wave-front sensor of the adaptive system has qualitatively the form shown in Fig. 14. It has a rather narrow allowable range of variation of the local wave front curvature. In a wide range of variation of the local curvature, we observe the repeated alternation of the signal sign at the constant sign of the local wave front curvature. This is likely explained by the mirror shape, varying under the effect of deformations, created by an individual actuator.⁴

The alternation of the signal sign is also observed at the constant curvature, but with the total wave front tilt varying in a narrow range. However, if the observed local area of the wave front is plane, then even in the presence of the total wave front tilt the signal from the corresponding detector is zero. Theoretically, such a behavior of the modulation characteristic for type I adaptive optical systems with the variation of the total tilt was predicted in Ref. 5. Upon the closure of the type I adaptive multidither system with spatially separated channels, it was almost impossible to achieve stable operation.

Thus, it has been found experimentally that wave-front sensors in type I adaptive optical systems can be considered as curvature sensors.

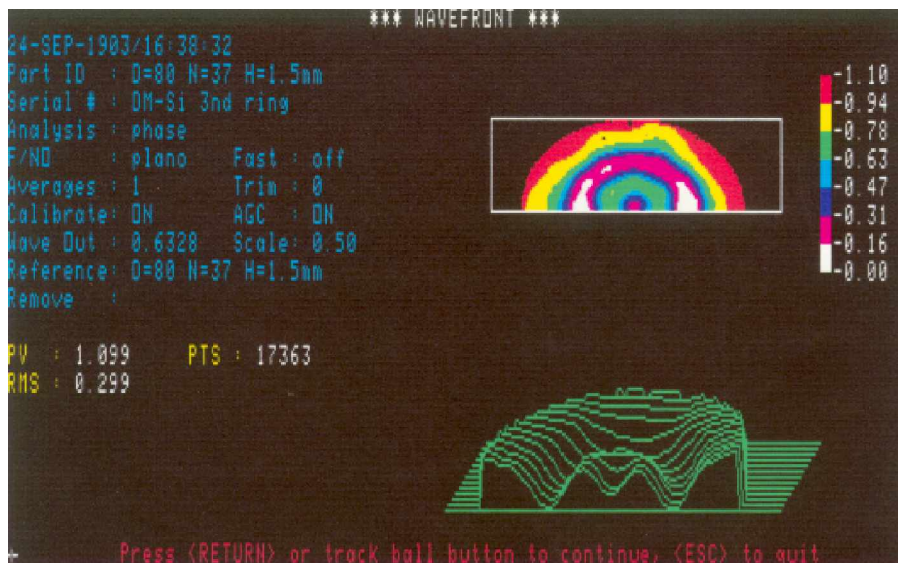


Fig. 13. Shape of the deformable mirror surface with the modulating voltage applied to shorter sections of its actuators.

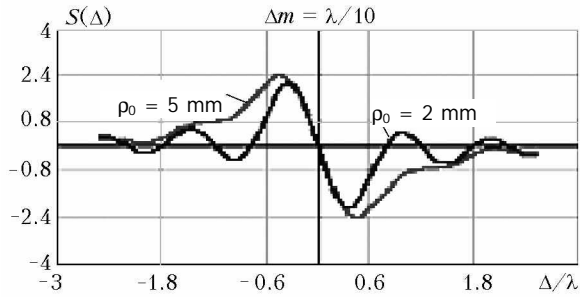


Fig. 14. Modulation characteristic for wave-front sensor of the type I adaptive optical system.

4.2. Type II adaptive optical systems

In investigating the type II multidither adaptive optical systems with spatially separated channels, the Newtonian phase modulator was used. It should be noted that due to only small range, in which the optical properties of this modulator vary, some typical features of type I adaptive optical systems are also characteristic of this modulator, as well. The most significant among these features are the limited range of curvature variations, at which this modulator can be used in a closed system, and the influence of the total wave front tilt on the feedback sign.

In aligning the optics of the wave-front sensor, the contact zone was shifted from the focal plane of the sensor objective. In Ref. 5, it is shown that such

a shift is equivalent to addition of the spherical component of distortions to the wave front. In this way, we shifted the modulation characteristic of the sensor to the point, at which it intersects the abscissa without inflection.

Repeated alternations of the sign of the modulation characteristic are not typical for such a modulator. The experimental results qualitatively corresponded to the modulation characteristic shown in Fig. 3. Figure 15 depicts a series of consecutive frames, demonstrating the character of variation of the spot in the focal plane of a long-focus mirror at the correction of a static image. The first image in this figure corresponds to the image of a point for the open system. Each frame is accompanied by the surface (above the frame), showing the intensity distribution in the maximum poorly reflects the adaptation process, because it takes time, which is much shorter than the frame duration. Therefore, if the transparency of the optical filter in front of the CCD camera (see Fig. 6) is optimal for the light spot at the corrected wave front, the light spot for the distorted wave front practically is not detected. In this figure, more significant characteristics are the shape of the light spot and the appearance of the characteristic diffraction nucleus and diffraction fringes. Their changes from frame to frame are more clearly seen in Fig. 16, which shows the same, as in Fig. 15, series of the photos along with the lines of the intensity level.

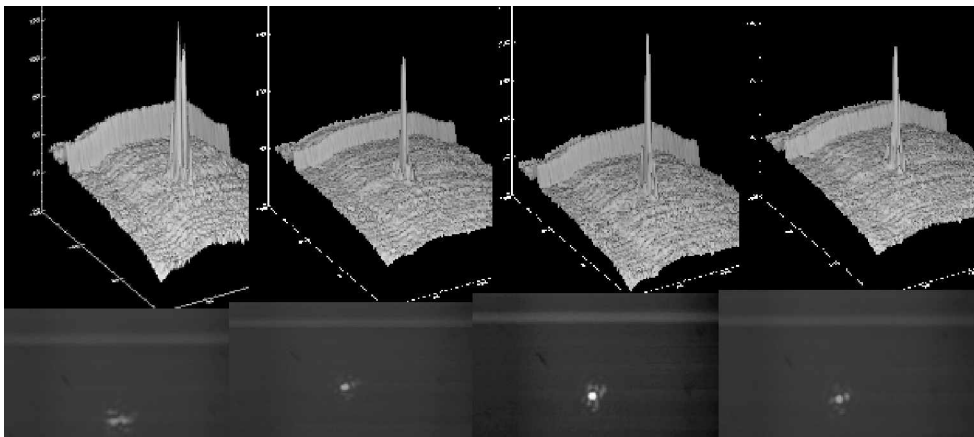


Fig. 15. Change of the spot shape on the detector located in the far zone.



Fig. 16. Level lines in the image intensity distribution in the focal plane for a series of images (see Fig. 15).

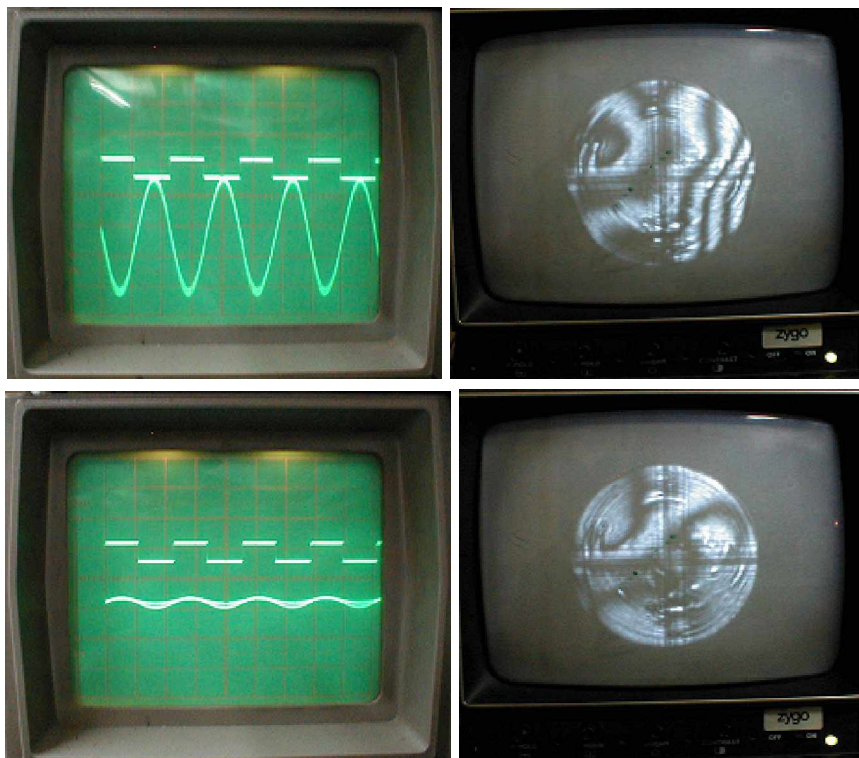


Fig. 17. Character of signals from a detector of an individual channel of the adaptive system and interferogram of the mirror surface before the correction of distortion and in the process of correction.

Figure 17 shows oscillograms of signals from the output of one channel of the adaptive system along with the interferograms of the mirror surface, recorded before and after the feedback was turned on.

Thus, the experiments showed that the logic of operation of the type II adaptive system with the Newtonian phase modulator corresponds qualitatively to the theoretical analysis from Ref. 5.

Conclusions

As a result of theoretical and experimental investigations of adaptive optical multidither systems with spatially separated channels, the following conclusions can be drawn:

1. Wave-front sensors in these adaptive systems are, essentially, curvature sensors.

2. Type I multidither adaptive optical systems, at the high sensitivity to wave front distortions, have

a small operating range and are very sensitive to errors in wave front tilt.

3. Type II adaptive optical systems with the Newtonian modulator, at the high sensitivity to wave front distortions, have a large dynamic range and are less sensitive to wave front tilts.

References

1. F. Roddier, *Adaptive Optics in Astronomy* (University Press, Cambridge, 1999).
2. A.B. Aleksandrov and P.P. Inshin, *Quant. Electron.* 22, No. 11, 1047–1050 (1992).
3. B.V. Prilepskii, A.N. Alikhanov, E.A. Berchenko, V.Yu. Kiselev, E.A. Narusbek, and A.S. Filatov (in press).
4. G. O'Meara, in: *Adaptive Optics*, ed. by E.A. Vitrichenko [Russian translation] (Mir, Moscow, 1980).
5. A.N. Alikhanov, B.V. Prilepskii, and A.S. Filatov, *Quant. Electron.* (in press).